Fe₃O₄-CuO Bimetallic Composite/Functionalized CNTs Modified Carbon Paste Electrode for Determination of Dexamethasone as a Doping Agent in Sports

Zhongyun Guo[*], *Haifeng Fan*

Department of Physical Education, Hebei GEO University, Shijiazhuang, 050031, China
[*]E-mail: guozhongyun1979@163.com

This study was carried out to fabricate bimetallic composite of Fe₃O₄-CuO nanoparticles and functionalized CNTs modified carbon paste electrode (Fe₃O₄-CuO@f-CNTs/CPE) for determination of dexamethasone (DXM) as a doping agent in sports. For synthesis of the modified electrode, Fe₃O₄ NPs and CuO NPs were synthesized using the hydrothermal method. The structural characterization of Fe₃O₄-CuO@f-CNTs/CPE using XRD and SEM showed that Cu NPs and Fe₃O₄ NPs were randomly entrapped on a porous structure of f-CNTs. The electrochemical studies using CV and amperometry exhibited that the wide range, sensitivity, stable and selective electrocatalytic responses to DXM were observed for Fe₃O₄-CuO@f-CNTs/CPE that related to high specific surface area nanocomposite, numerous active sites' exposure and synergetic effect of Fe₃O₄ and CuO NPs and f-CNTs. The linear range, sensitivity and limit of detection of sensor were obtained 0 to 3100 μM, 0.8665μA/μM and 0.003μM, respectively. The accuracy and applicability of Fe₃O₄-CuO@f-CNTs/CPE for determination of DXM was examined in medicinal and human body fluid samples and results showed the acceptable value of recovery (≥94.35 %) and RSD (≤3.71 %), indicating the prepared sensor can be used as a reliable DXM sensor in clinical specimens.

1. INTRODUCTION

Doping assigns to the use of banned substances in competitive sports and is an important issue for all athletes, coaches, managers, sports organizations and sports fans because it undermines the efforts of clean athletes deny others the ability to compete on a level playing field and damages the true spirit of competitive sport [1, 2]. It is also referred performance-enhancing drugs to improve the athletic performance and can have hurtful and long-lasting side effects such as irregular heart rhythm,

sudden death, elevated blood pressure, nose bleeds, heart attack, psychosis, sinusitis, tremor, dizziness, stroke, cancer and infertility [3, 4].

In general, World Anti-Doping Agency (WADA) have been banned some performance-enhancing drugs which contained street drugs, stimulants, anabolic steroids, peptide hormones, alcohol, beta-blockers, diuretics, gene manipulation, beta-2 agonists, blood doping, and anti-estrogens [5]. Therefore, athletes who participate in sports are subject to accidental in and out of race testing [6, 7]. Testing can be done on blood and/or urine samples dependent on the substances being verified. The type and frequency of testing differ between sport based upon various factors containing doping history in the sport, duration of the season, substances being taken, and type of sports [8, 9].

Dexamethasone (DXM, $C_{22}H_{29}FO_5$, (8S,9R,10S,11S,13S,14S,16R,17R)-9-fluoro-11,17-dihydroxy-17-(2-hydroxyacetyl)-10,13,16-trimethyl-6,7,8,11,12,14,15,16-octahydrocyclopenta[a]phenanthren-3-one) as glucocorticoid medication to relieve inflammation in various parts of the body is listed as the performance-enhancing steroid in the WADA 2019 list of forbidden drugs and has been defined as a stated substance attracting a sentence if found in an athlete's body system [10, 11]. DXM as a systemic corticosteroid and long-acting shows the potency around 25-times larger than short-acting product [12]. It is generally available and most athletes resorting to doping consume it hours before their competition to improve performance [13]. It has the potential to increase sport performances to help athletes in high altitudes [14, 15].

Therefore, many studies have been conducted for the determination of DXM using high performance liquid chromatography, capillary electrophoresis, chemical ionization–mass spectrometry, gas chromatography, chemometric, and electrochemistry [16-22]. Among these methods, electrochemical techniques are fast and low-cost and potentially provide the ability to improve the sensor properties [23-27]. The recent progress in fabrication and application of the nanostructured electrode materials based sensors in fluid environments have been indicated that the high volume ratio and large specific surface area of the nanomaterials and nanocomposites allow improving the catalytic, absorption, interaction and sensing response by the rapid movement of analytes through nanomaterials-based sensors [28]. Therefore, this study was carried out to fabrication of bimetallic composite of Fe_3O_4-CuO and f-CNTs for determination of dexamethasone as a doping agent in sports.

2. MATERIALS AND METHOD

2.1. The synthesis of Fe₃O₄-CuO@f-CNT modified CPE

For prepare the *CPE*, the uniform mixture of graphite powder (99%, Qingdao Furuite Graphite Co., Ltd., China) and paraffin oil (7:3 w/w) were provided less than 35°C and packed into a hollow Teflon-tube electrode (0.3 mm diameter) which is equipped with copper as electrical contact.

Fe_3O_4 NPs and CuO NPs were synthesized using the hydrothermal method [29, 30]. For the synthesis of Fe_3O_4 NPs, 4 g $FeCl_3$ (99%, Merck, Germany), 0.5 g natriumaceticum (≥99%, Sigma-Aldrich) and 0.5 g sodium citratedihydrate (≥99%, Sigma-Aldrich) were dissolved in 100 mL ethylene glycolanhydrous (99.8%, Sigma-Aldrich) under the magnetic string, and the resulted mixture was

moved in the oven at 180 °C for 24 hours. To obtain CuO NPs, 5g $Cu(NO_3)_2 \cdot 3H_2O$ (99%, Merck, Germany) and 0.1 g $N_2H_4.H_2O$ (64%, Sigma-Aldrich) and 0.5 g $NaBH_4$ (99%, Sigma-Aldrich) were dissolved in 10 mL deionized water under the magnetic string and the resulted mixture was moved in oven at 160 °C for 10 hours.

For preparing Fe_3O_4-CuO@f-CNT nanocomposites modified CPE, CNTs (99%, Jiaxing ACG Composites Co., Ltd., China) were ultrasonically functionalized in a mixture of sulfuric acid (97%, Merck, Germany) and nitric acid (69%, Merck, Germany) (3:1 v/v) at 80°C for 4 hours [1]. Next, the functionalized CNTs (f-CNTs) were washed with deionized water and then filtrated and dispersed in ethanol (>99%, Merck, Germany). After that, the dispersed f-CNTs was dried at 50°C for 12 hours and collected. 1 g of prepared f-CNTs, 1 g of CuO NPs and 1 g of Fe_3O_4 NPs were ultrasonically dispersed in deionized water, and centrifuged at 1000 rpm for 6 minutes. The resulted supernatant was removed and 0.1 ml of the resulted precipitates was slowly dropped on CPE surface and the CPE was dried in the oven at room temperature.

2.2. Real sample preparation

DXM 4 mg tablets were provided from a local pharmacy. 10 tablets were ultrasonically dissolved in 40 ml of 0.1 M PBS which was applied as a real medicinal sample (4 mg/ml DXM solution). In order to prepare the human serum sample, the DXM-free human serum sample was taken from Capital Medical University Beijing Hospital of Traditional Chinese Medicine (Beijing, China) and was treated with 1 mL methanol as a protein precipitating agent for 15 minutes. Afterward, the sample was centrifuged at 1500 rpm for 5 minutes. The resulted in precipitates were removed and the resulted supernatant was filtered and was diluted to 100ml with the 0.1 M PBS. The standard addition method was applied to analytical studies of real samples.

2.3. Characterization

Cyclic voltammetry (CV) and amperometry analysis were conducted on AUTO LAB Potentiostat (Eco Chemie, PGSTAT 302, Utrecht, and The Netherlands) in the three-electrode electrochemical cell which enclosed Ag/AgCl, Pt wire and modified CPE as the reference, counter and working electrode, respectively. 0.1M PBS pH 7.0 was used as an electrolyte in electrochemical studies that it was prepared from 0.1M NaH_2PO_4 (99%, Sigma-Aldrich) and 0.1M Na_2HPO_4 (99.95%, Sigma-Aldrich).

The crystal structure and morphological of modified electrodes were studied through X-ray diffraction (XRD, X'pert MPD, Philips, Eindhoven, the Netherlands) and scanning electron microscopy (SEM), respectively.

Int. J. Electrochem. Sci., 16 (**2021**) Article Number: 211125

4

3. RESULTS AND DISCUSSION

The morphology of the surface of f-CNTs/CPE and Fe_3O_4-CuO@f-CNTs/CPE are presented in Figure 1. As seen in Figure 1a, f-CNTs/CPE is covered of CNTs which homogeneously spreads on the CPE surface with a diameter of 70nm. The tubes structure of the f-CNTs bundle forms a 3D porous network and presents a large effective surface area. Figure 1b shows a random entrapped Cu NPs and Fe_3O_4 NP on f-CNTs. The porous structure of f-CNTs facilitates the fixing of the metal NPs on electrode surface. The negative charges on the surface of CNTs and functional groups such as hydroxyl and carboxyl groups on f-CNTs improve the capability to interact with Cu NPs and Fe_3O_4 NPs [31]. The average diameter of metal NPs is ∼45 nm.
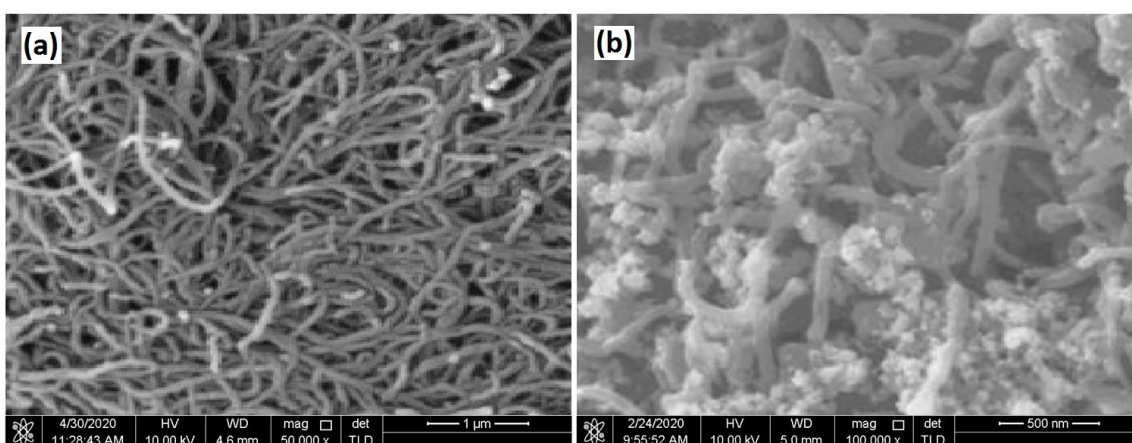
Figure 1. FESEM image of (a) f-CNTs/CPE and (b) Fe_3O_4-CuO@f-CNTs/CPE

XRD patterns of powders of f-CNTs and Fe_3O_4/f-CNTs, CuO/f-CNTs and Fe_3O_4-CuO@f-CNTs are displayed in Figure 2. All XRD patterns show two sharp diffraction peaks at 25.90°and 44.03° that it corresponded to (002) and (100) graphitic planes, respectively [32]. XRD pattern of Fe_3O_4/f-CNTs shows the additional peaks at 17.98°, 30.09°,35.40°,53.71°,57.25°, 62.81° and 74.56° which assigned to (111), (220), (311), (422), (511), (440), and (533) diffraction planes of Fe_3O_4 in the cubic spinel crystal structure (JCPDS card no. 85-1436). Figure 2c exhibits the XRD patterns of CuO/f-CNTs composite that it shows the characteristic peak of cubic phase of CuO at 36.11°, 42.05°, 61.29°, and 74.81° which related to the (111), (200), (220), and (311) planes, respectively (JPCDS no. 78–0428). The XRD pattern of Fe_3O_4-CuO@f-CNTs from Figure 2d shows the (111), (220), (311),(422), (511), (440), and (533) planes of Fe_3O_4 and (200) and (220) planes of cubic phase of CuO. These results confirm that the nanocomposite of Fe_3O_4-CuO@f-CNTs have been successfully synthesized using the hydrothermal method.
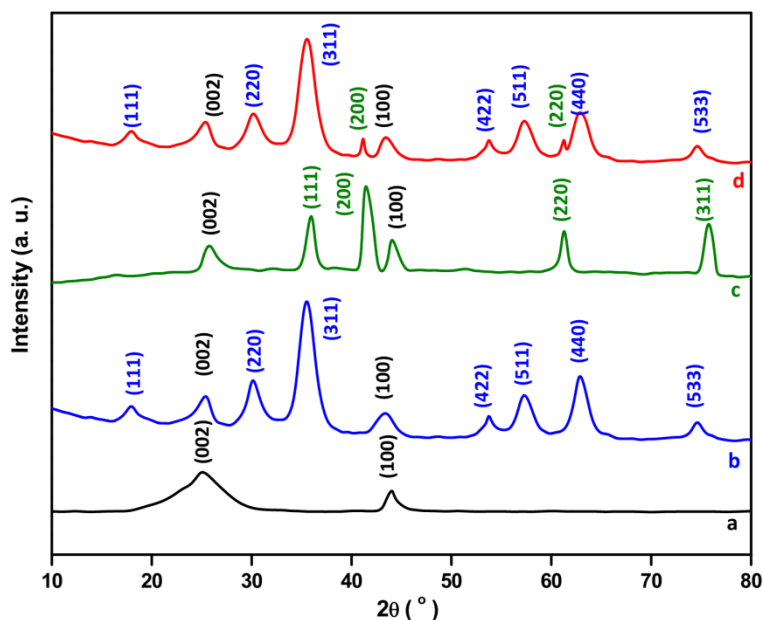
Figure 2. XRD pattern of powders of (a) f-CNTs and (b) Fe$_3$O$_4$/f-CNTs, (c) CuO/f-CNTs and (d) Fe$_3$O$_4$-CuO@f-CNTs

The electrochemical responses of CPE, f-CNTs/CPE, Fe$_3$O$_4$/f-CNTs/CPE, CuO/f-CNTs/CPE and Fe$_3$O$_4$-CuO@f-CNTs/CPE were examined at a scan rate of 10 mV/s in 0.1 M PBS pH 7.0 containing 1 μM DXM. Figure 3a shows the CV response of CPE does not show any peak. As observed, f-CNTs/CPE, Fe$_3$O$_4$/f-CNTs/CPE, CuO/f-CNTs/CPE and Fe$_3$O$_4$-CuO@f-CNTs/CPE show electrocatalytic response to the presence of DXM at the potential of 0.64, 0.64, 0.67 and 0.63 V, respectively which attributed to oxidation of DXM [33]. The higher electrocatalytic response is observed for Fe$_3$O$_4$-CuO@f-CNTs/CPE that it related to high specific surface area nanocomposite, numerous active sites' exposure and synergetic effect of Fe$_3$O$_4$ and CuO NPs and f-CNTs [34]. Fe$_3$O$_4$ nanostructures shows mechanical and chemical instability, week electrical conductivity, and poor electrocatalytic activity, and combination the Fe$_3$O$_4$ with CuO NPs and f-CNTs effectively promotes mechanical properties, electrical conductivity and specific surface area [35]. Moreover, unique structural of f-CNTs can form bridge defects to enhance electron transfer between the electrode surface and electrolyte and improve mass transport kinetics [36, 37]. Thus, Fe$_3$O$_4$-CuO@f-CNTs composite causes to form of large contact area, and coupling effects both of metallic nanoparticles via the electron interaction significantly optimize the electronic structure modulation which increases the density of charge carriers around the Fermi level [34, 38]. Therefore, Fe$_3$O$_4$-CuO@f-CNTs/CPE was selected for the following electrochemical studies.

The stability of electrochemical response of Fe$_3$O$_4$-CuO@f-CNTs/CPE was studied. Figure 4 depicts initial and 80th recorded CVs in presence of 1 μM DXM which indicated to 3 % change for electrocatalytic current. It evidence to high stability response of Fe$_3$O$_4$-CuO@f-CNTs/CPE for determination of DXM that it can be related to covalent surface modification strategy and distribution of oxygen-containing functional groups at the open ends and sidewalls of CNTs which facilitate the binding, embedding and loading metallic nanoparticles on the surface of nanotubes, and form foothold

functional groups as attachment points for Fe_3O_4-CuO nanoparticle and larger absorbance of the analyte [39].
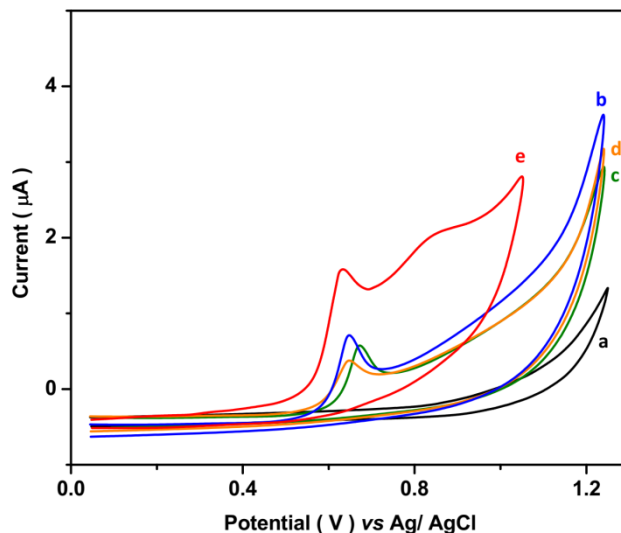

Figure 3. CV responses of (a) CPE, (b) f-CNTs/CPE, (c) Fe_3O_4/f-CNTs/CPE, (d) CuO/f-CNTs/CPE and (e) Fe_3O_4-CuO@f-CNTs/CPE at a scan rate of 10 mV/s in 0.1 M PBS pH 7.0 containing 1 µM DXM.
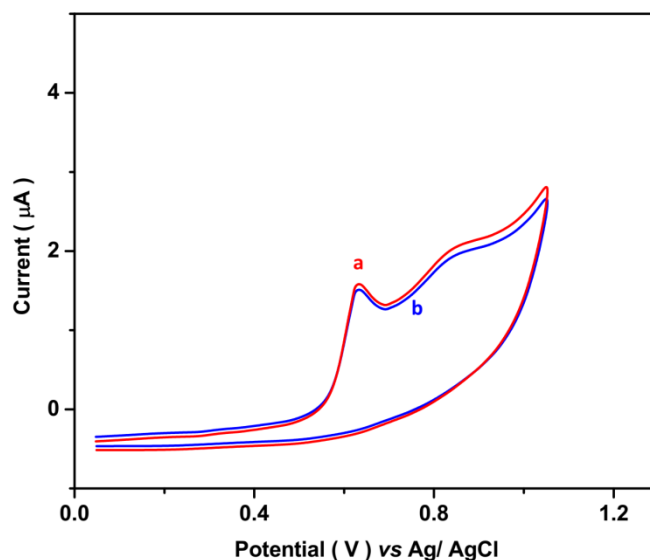
Figure 4. (a) initial and (b) 80th recorded CVs of response of Fe_3O_4-CuO@f-CNTs/CPE at a scan rate of 10 mV/s in 0.1 M PBS pH 7.0 containing 1 µM DXM.

Further electrochemical studies were conducted through the amperometry technique for the determination of sensing properties of Fe_3O_4-CuO@f-CNTs/CPE as DXM sensor. Figure 5 displays the amperometry response of the proposed sensor and the resulted calibration curve in 0.1M PBS at 0.63V and 1500 rpm rotating speed to the addition of 100µM DXM. The fast response of sensor can be

observed after each addition of 100 μM DXM solution. As seen, the amperometric current is linearly increased with the addition of DXM solution from 0 to 3100 μM. The sensitivity and detection limit of sensor are estimated at 0.8665μA/μM and 0.003 μM, respectively. The obtained sensing properties of Fe_3O_4-CuO@f-CNTs/CPE are compared by the reported DXM sensor in Table 1. As observed, Fe_3O_4-CuO@f-CNTs/CPE exhibit wide linear range for the determination of DXM that is associated with distribution of oxygen-containing functional groups on CNTs that it forms the defect and nanostructured substrate for anchoring the metallic nanoparticles which provide numerous absorbing sites on Fe_3O_4-CuO@f-CNTs/CPE.
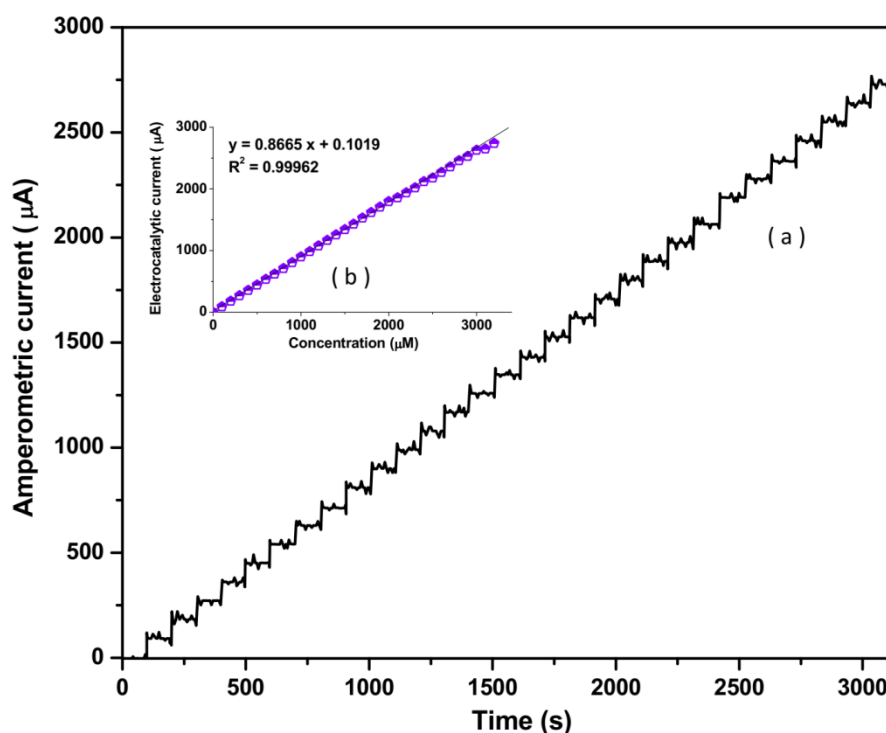
Figure 5. (a) Amperometry response of Fe_3O_4-CuO@f-CNTs/CPE and (b) the resulted calibration curve in 0.1M PBS at 0.63V and 1500 rpm rotating speed to the addition of 100μM DXM.

Table 1. Comparison between the sensing properties of Fe3O4-CuO@f-CNTs/CPE and other reported DXM sensor in literatures.

Electrode	Technique	Linear Range (μM)	limit of detection (μM)	Ref.
Fe_3O_4-CuO@f-CNTs/CPE	Amperometry	0-3100	0.003	This work
Fe_3O_4/PANI–Cu II microsphere/carbon ionic liquid electrode	DPV	50-3000	0.003	[40]
α-Fe_2O_3/graphene oxide	DPV	0.1–50	0.076	[41]
β-cyclodextrin /CPE	DPV	0.41 - 20	0.36	[42]

|				
Hanging mercury drop electrode	SWP	0.009-0.4	0.003	[43]
Dropping mercury electrode	DPP	25.5-122.3	7.6	[42]
MWCNTs/Pencil Electrode	SWV	0.15-100	0.09	[44]
Fullerene-C$_{60}$-modified edge plane pyrolytic graphite electrode	OSWV	0.05–100	0.055	[45]
Amalgam film silver based electrode	CV	0.0025-0.225	0.1	[46]

DPV: Differential pulse voltammetry; SWP: Square wave polarography; DPP: Differential pulse polarography; SWV: Square wave voltammetry; OSWV: Osteryoung square wave voltammetry.

The selectivity and interference response of Fe$_3$O$_4$-CuO@f-CNTs/CPE as DXM sensor were investigated in presence of interferents. Table 2 shows the resulted amperometric currents of Fe$_3$O$_4$-CuO@f-CNTs/CPE in 0.1M PBS at 0.63V in 1µM successive additions of DXM solution and 10 µM of various interferents. Results indicate that the response of the modified electrode toward the addition of DXM is significantly higher than that toward the addition of the interferents, implying the selective response of modified electrode and substances in Table 2 did not interfere with the results of DXM amperometric determination.

Table 2. The resulted amperometric currents of Fe$_3$O$_4$-CuO@f-CNTs/CPE in 0.1M PBS at 0.63V in 1µM successive additions of DXM and 10µM of different interferents.

substance	Concentration (µM)	Amperometric current density (µA) at 0.63 V	RSD (%)
DXM	1	0.8671	±0.0091
Mg^{2+}	10	0.0153	±0.0018
Ca^{2+}	10	0.0192	±0.0008
NO$_3^-$	10	0.0187	±0.0009
SO$_4^{2-}$	10	0.0210	±0.0022
CO$_3^{2-}$	10	0.0281	±0.0028
Ascorbic acid	10	0.0200	±0.0018
Uric acid	10	0.0289	±0.0037
Citric acid	10	0.0308	±0.0072
Xanthine	10	0.0277	±0.0044
Urea	10	0.0214	±0.0052
Albumin	10	0.0134	±0.0021
Phenazopyridine	10	0.0277	±0.0022
Hypoxanthine	10	0.0101	±0.0027
Methyprednisolone	10	0.0106	±0.0004
Glucose	10	0.0202	±0.0008
Amoxicilin	10	0.0275	±0.0051
Cortion	10	0.0109	±0.0007
Dopamine	10	0.0211	±0.0012

The accuracy and applicability of Fe_3O_4-CuO@f-CNTs/CPE to the determination of DXM were examined in medicinal and human body fluid samples. For the study, the prepared real medicinal sample of DXM tablets, the amperometry experiments were performed using Fe_3O_4-CuO@f-CNTs/CPE in prepared real sample with 0.1M PBS at 0.63 V in successive additions of DXM solution. Figure 6 exhibits the amperometry response and an obtained calibration plot, implying the DXM content in prepared sample is 3.78 mg/ml that it is very close to DXM concentration in the prepared real sample of tablets (4mg/ml).
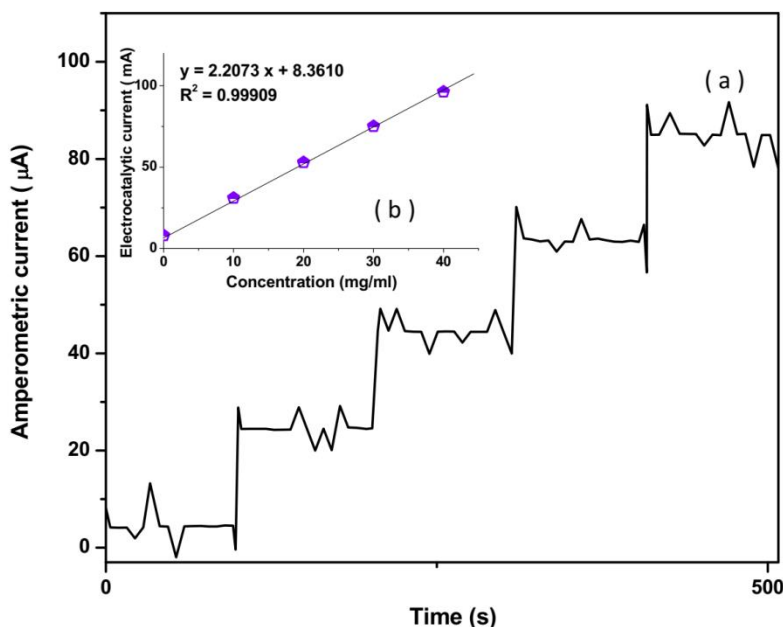
Figure 6. (a) Amperometry response of Fe_3O_4-CuO@f-CNTs/CPE and (b) the achieved calibration plot of Fe_3O_4-CuO@f-CNTs/CPE in prepared real sample of DXM tablets with 0.1M PBS at 0.63V in successive addition of DXM solution.

Table 3. Analytical findings of Fe_3O_4-CuO@f-CNTs/CPE to determine DXM in prepared real specimens of DXM tablets and human serum.

Sample	Added(mg/ml)	Found(mg/ml)	Recovery (%)	RSD (%)
DXM tablets	0.00	3.78	-	-
	10.00	13.73	99.50	3.18
	20.00	22.65	94.35	3.44
	30.00	33.68	99.66	2.89
	40.00	42.70	97.30	3.73
Human serum	0.00	0.00	-	-
	10.00	9.92	99.20	2.84
	20.00	19.90	99.50	3.28
	30.00	28.91	96.36	3.71
	40.00	39.18	97.95	3.39

In addition, it can be found from Table 3, the obtained values for recovery (≥94.35 %) and RSD (≤3.73 %) for the prepared real samples of DXM tablets is acceptable. Analytical applicability of sensor was studied in the preparation of DXM-free human serum and results show that it was not detected DXM the real sample of serum. Table 3 also shows the analytical results, indicating to acceptable values of recovery (≥96.36 %) and RSD (≤3.71 %). Therefore, Fe_3O_4-CuO@f-CNTs/CPE can be used as reliable DXM sensor in clinical specimens.

4. CONCULUSION

This study presented the hydrothermal synthesis of Fe_3O_4 and CuO NPs*,* and a composite of Fe_3O_4-CuO@f-CNTs/CPE for the determination of DXM as a doping agent in sports. Results of structural characterization showed that Cu NPs and Fe_3O_4 NP was randomly entrapped on porous structure f-CNTs. Results of electrochemical studies showed that the broad range, stable and selective electrocatalytic response to DXM were observed for Fe_3O_4-CuO@f-CNTs/CPE. The linear range, sensitivity and limit of detection of the sensor were obtained 0 to 3100 µM, 0.8665µA/µM and 0.003 µM, respectively. The applicability of Fe_3O_4-CuO@f-CNTs/CPE to the determination of DXM were examined in medicinal and human body fluid samples and results showed the acceptable value of RSD and recovery, implying the prepared sensor can be used as a reliable DXM sensor in clinical specimens.

References

1. Y. Wang, C. Li, Y. Zhang, M. Yang, B. Li, D. Jia, Y. Hou and C. Mao, *Journal of Cleaner Production*, 127 (2016) 487.
2. Y. Orooji, B. Tanhaei, A. Ayati, S.H. Tabrizi, M. Alizadeh, F.F. Bamoharram, F. Karimi, S. Salmanpour, J. Rouhi and S. Afshar, *Chemosphere*, 281 (2021) 130795.
3. H. Guan, S. Huang, J. Ding, F. Tian, Q. Xu and J. Zhao, *Acta Materialia*, 187 (2020) 122.
4. H. Savaloni, E. Khani, R. Savari, F. Chahshouri and F. Placido, *Applied Physics A*, 127 (2021) 1.
5. Z. Savari, S. Soltanian, A. Noorbakhsh, A. Salimi, M. Najafi and P. Servati, *Sensors and Actuators B: Chemical*, 176 (2013) 335.
6. M. Zhang, L. Zhang, S. Tian, X. Zhang, J. Guo, X. Guan and P. Xu, *Chemosphere*, 253 (2020) 126638.
7. H. Karimi-Maleh, Y. Orooji, F. Karimi, M. Alizadeh, M. Baghayeri, J. Rouhi, S. Tajik, H. Beitollahi, S. Agarwal and V.K. Gupta, *Biosensors and Bioelectronics*, 184 (2021) 113252.
8. K. Yang, Q. Liu, Y. Zheng, H. Yin, S. Zhang and Y. Tang, *Angewandte Chemie*, 133 (2021) 6396.
9. Z. Li, M. Peng, X. Zhou, K. Shin, S. Tunmee, X. Zhang, C. Xie, H. Saitoh, Y. Zheng and Z. Zhou, *Advanced Materials*, (2021) 2100793.
10. X. Zhang, X. Sun, T. Lv, L. Weng, M. Chi, J. Shi and S. Zhang, *Journal of Materials Science: Materials in Electronics*, 31 (2020) 13344.
11. G. Luo, Q. Zhang, M. Li, K. Chen, W. Zhou, Y. Luo, Z. Li, L. Wang, L. Zhao and K.S. Teh, *Nanotechnology*, 32 (2021) 405402.
12. M. Zhang, X. Song, X. Ou and Y. Tang, *Energy Storage Materials*, 16 (2019) 65.

13. X. Wang, Z. Feng, B. Xiao, J. Zhao, H. Ma, Y. Tian, H. Pang and L. Tan, *Green Chemistry*, 22 (2020) 6157.
14. H. Cheng, T. Li, X. Li, J. Feng, T. Tang and D. Qin, *Journal of The Electrochemical Society*, 168 (2021) 087504.
15. H. Karimi-Maleh, M.L. Yola, N. Atar, Y. Orooji, F. Karimi, P.S. Kumar, J. Rouhi and M. Baghayeri, *Journal of colloid and interface science*, 592 (2021) 174.
16. D. Courtheyn, J. Vercammen, H. De Brabander, I. Vandenreyt, P. Batjoens, K. Vanoosthuyze and C. Van Peteghem, *Analyst*, 119 (1994) 2557.
17. E.T. Mallinson, J.S. Dreas, R.T. Wilson and A.C. Henry, *Journal of Agricultural and Food Chemistry*, 43 (1995) 140.
18. S. Duarah, M. Sharma and J. Wen, *Journal of Chromatography B*, 1170 (2021) 122609.
19. A.J. Nepote, P.C. Damiani and A.C. Olivieri, *Journal of pharmaceutical and biomedical analysis*, 31 (2003) 621.
20. S. Tahir, K. Yasmeen, M. Hanif, O. Khaliq, H. Muhammad, I.A.T. Hafsa, S. Jahangir and S.T. Ali, *International Journal of Electrochemical Science* 14 (2019) 5748.
21. H. Karimi-Maleh, Y. Orooji, A. Ayati, S. Qanbari, B. Tanhaei, F. Karimi, M. Alizadeh, J. Rouhi, L. Fu and M. Sillanpää, *Journal of Molecular Liquids*, 329 (2021) 115062.
22. F. Chahshouri, H. Savaloni, E. Khani and R. Savari, *Journal of Micromechanics and Microengineering*, 30 (2020) 075001.
23. R. Abdi, A. Ghorbani-HasanSaraei, H. Karimi-Maleh, S.N. Raeisi and F. Karimi, *International Journal of Electrochemical Science* 15 (2020) 2539.
24. Y. Feng, Y. Liu, B. Feng, H. Chen, L. You and H. Pei, *International Journal of Electrochemical Science* 16 (2021) 210812.
25. Y. Chen, D. Wei, K. He, H. Li and F. Sun, *International Journal of Electrochemical Science* 16 (2021) 210522.
26. H. Karimi-Maleh, M. Alizadeh, Y. Orooji, F. Karimi, M. Baghayeri, J. Rouhi, S. Tajik, H. Beitollahi, S. Agarwal and V.K. Gupta, *Industrial & Engineering Chemistry Research*, 60 (2021) 816.
27. R. Savari, H. Savaloni, S. Abbasi and F. Placido, *Sensors and Actuators B: Chemical*, 266 (2018) 620.
28. M. Rizwan, N.F. Mohd-Naim and M.U. Ahmed, *Sensors*, 18 (2018) 166.
29. C. Lou, T. Jing, J. Tian, Y. Zheng, J. Zhang, M. Dong, C. Wang, C. Hou, J. Fan and Z. Guo, *Journal of Materials Research*, 34 (2019) 2964.
30. K. Giannousi, E. Hatzivassiliou, S. Mourdikoudis, G. Vourlias, A. Pantazaki and C. Dendrinou-Samara, *Journal of inorganic biochemistry*, 164 (2016) 82.
31. S. Liang, G. Li and R. Tian, *Journal of Materials Science*, 51 (2016) 3513.
32. Y.-S. Li, J.-L. Liao, S.-Y. Wang and W.-H. Chiang, *Scientific Reports*, 6 (2016) 22755.
33. S. Alimohammadi, M.A. Kiani, M. Imani, H. Rafii-Tabar and P. Sasanpour, *Scientific Reports*, 9 (2019) 11775.
34. Y. Gao, N. Zhang, C. Wang, F. Zhao and Y. Yu, *ACS Applied Energy Materials*, 3 (2019) 666.
35. R. Madhuvilakku, S. Alagar, R. Mariappan and S. Piraman, *Sensors and Actuators B: Chemical*, 253 (2017) 879.
36. Z. Zhao, W. Wang, W. Tang, Y. Xie, Y. Li, J. Song, S. Zhuiykov, J. Hu and W. Gong, *Ionics*, (2019) 1.
37. C. Lee, S.H. Lee, M. Cho and Y. Lee, *Microchimica Acta*, 183 (2016) 3285.
38. W. Huang, C. Peng, J. Tang, F. Diao, M. Nulati Yesibolati, H. Sun, C. Engelbrekt, J. Zhang, X. Xiao and K.S. Mølhave, *Journal of Energy Chemistry*, 65 (2022) 78.
39. K.A. Wepasnick, B.A. Smith, K.E. Schrote, H.K. Wilson, S.R. Diegelmann and D.H. Fairbrother, *Carbon*, 49 (2011) 24.
40. A. Fatahi, R. Malakooti and M. Shahlaei, *RSC Advances*, 7 (2017) 11322.

41.   M. Mazloum-Ardakani, N. Sadri and V. Eslami, *Electroanalysis*, 32 (2020) 1148.
42.   K. Balaji, G.R. Reddy, T.M. Reddy and S.J. Reddy, *African Journal of Pharmacy and Pharmacology*, 2 (2008) 157.
43.   E.M. Ghoneim, M.A. El-Attar and M.M. Ghoneim, *Journal of AOAC International*, 92 (2019) 597.
44.   B. Rezaei, S. Zare and A.A. Ensafi, *Journal of the Brazilian Chemical Society*, 22 (2011) 897.
45.   R.N. Goyal, V.K. Gupta and S. Chatterjee, *Biosensors and Bioelectronics*, 24 (2009) 1649.
46.   J. Smajdor, R. Piech and B. Paczosa-Bator, *Journal of Electroanalytical Chemistry*, 809 (2018) 147.